

AD-A117 363

DAVID W TAYLOR NAVAL SHIP RESEARCH AND DEVELOPMENT CE--ETC F/G 1/3  
LIFT SYSTEM AND FAN PERFORMANCE OF AIR CUSHION SUPPORTED VEHICLE--ETC(U)  
FEB 82 D D MORAN, A N JENNINGS

UNCLASSIFIED

DTNSRDC/SPD-0695-02

NI

1 1 1  
1 1 1  
1 1 1

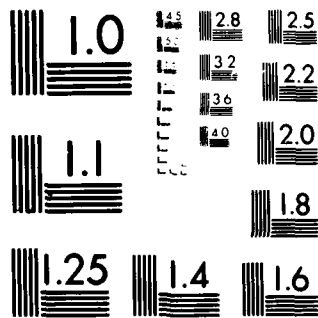
END

DATE

FILED

08-82

DTIC



MICROCOPY RESOLUTION TEST CHART  
NATIONAL BUREAU OF STANDARDS 1963-A

AD A117363

DTNSRDC/SPD-0695-02

5

**DAVID W. TAYLOR NAVAL SHIP  
RESEARCH AND DEVELOPMENT CENTER**

Bethesda, Maryland 20084



**LIFT SYSTEM AND FAN PERFORMANCE OF  
AIR CUSHION SUPPORTED VEHICLES**

by

D.D. MORAN

and

A.N. JENNINGS

**DTIC  
SELECTE  
JUL 23 1982  
H**

APPROVED FOR PUBLIC RELEASE: DISTRIBUTION UNLIMITED

SHIP PERFORMANCE DEPARTMENT

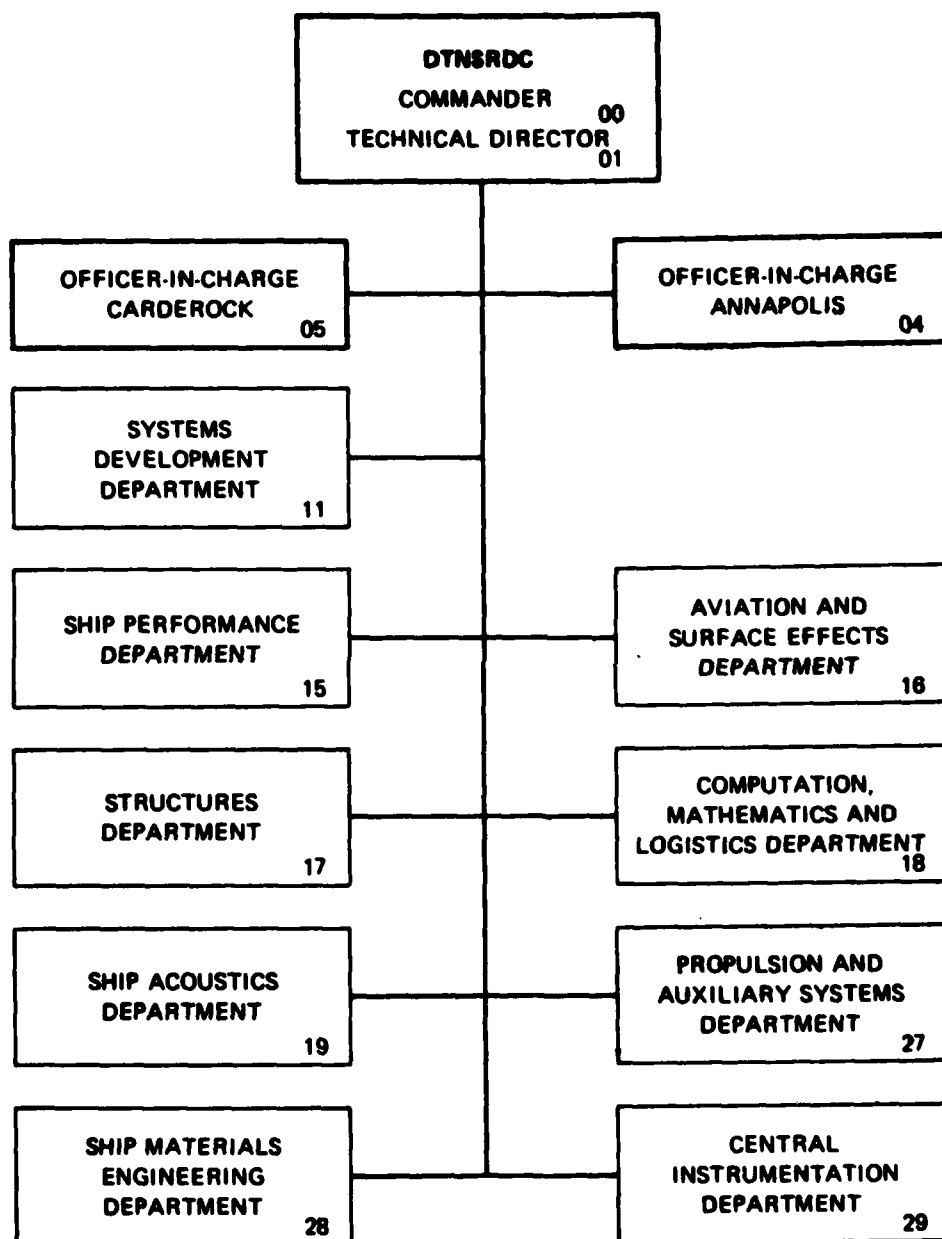
FEBRUARY 1982

DTNSRDC/SPD-0695-02

**DTIC FILE COPY**

LIFT SYSTEM AND FAN PERFORMANCE OF  
AIR CUSHION SUPPORTED VEHICLES

## MAJOR DTNSRDC ORGANIZATIONAL COMPONENTS



UNCLASSIFIED

SECURITY CLASSIFICATION OF THIS PAGE (When Data Entered)

REPORT DOCUMENTATION PAGE		READ INSTRUCTIONS BEFORE COMPLETING FORM
1. REPORT NUMBER  DTNSRDC/SPD-0695-02	2. GOVT ACCESSION NO.  ADA117 363	3. RECIPIENT'S CATALOG NUMBER
4. TITLE (and Subtitle)  LIFT SYSTEM AND FAN PERFORMANCE OF AIR CUSHION SUPPORTED VEHICLES		5. TYPE OF REPORT & PERIOD COVERED
7. AUTHOR(s)  D.D. MORAN A.N. JENNINGS		6. PERFORMING ORG. REPORT NUMBER
9. PERFORMING ORGANIZATION NAME AND ADDRESS  David W. Taylor Naval Ship R&D Center Code 1562 ethesda, MD 20084		8. CONTRACT OR GRANT NUMBER(s)
11. CONTROLLING OFFICE NAME AND ADDRESS  Amphibious Assault Landing Craft Office Systems Development Department David W. Taylor Naval Ship R&D Center		10. PROGRAM ELEMENT, PROJECT, TASK AREA & WORK UNIT NUMBERS Task Area S 1417 Task 14174 Work Unit No. 1180-750
14. MONITORING AGENCY NAME & ADDRESS (if different from Controlling Office)		12. REPORT DATE  February 1982
		13. NUMBER OF PAGES  37
		15. SECURITY CLASS. (of this report)  Unclassified
		15a. DECLASSIFICATION/DOWNGRADING SCHEDULE
16. DISTRIBUTION STATEMENT (of this Report)  APPROVED FOR PUBLIC RELEASE: DISTRIBUTION UNLIMITED		
17. DISTRIBUTION STATEMENT (of the abstract entered in Block 20, if different from Report)		
18. SUPPLEMENTARY NOTES		
19. KEY WORDS (Continue on reverse side if necessary and identify by block number)  ACV, ACV Lift System, ACV Fans, Fan Failures		
20. ABSTRACT (Continue on reverse side if necessary and identify by block number) An analysis of the AALC JEFF lift systems and fans from the viewpoints of performance and structural design is performed. A summary of performance data related to the JEFF lift systems is presented, and suggested approaches for JEFF (A) lift fan design, for which these data provided the baseline information, are provided. Published methods of scaling fan performance data from model to full-scale are evaluated. Finally, the structural design characteristics of the JEFF fans are discussed.		

DD FORM 1 JAN 73 1473

EDITION OF 1 NOV 65 IS OBSOLETE  
S/N 0102-LF-014-4601

UNCLASSIFIED

SECURITY CLASSIFICATION OF THIS PAGE (When Data Entered)

SECURITY CLASSIFICATION OF THIS PAGE (When Data Entered)

SECURITY CLASSIFICATION OF THIS PAGE (When Data Entered)

## TABLE OF CONTENTS

	Page
LIST OF FIGURES . . . . .	111
ABSTRACT. . . . .	1
ADMINISTRATIVE INFORMATION. . . . .	1
INTRODUCTION. . . . .	1
LIFT SYSTEM PERFORMANCE ANALYSIS. . . . .	2
JEFF (A) FAN PERFORMANCE. . . . .	5
DESIGN REQUIREMENTS. . . . .	5
APPROACHES TO A NEW DESIGN . . . . .	6
OBSERVATIONS AND RECOMMENDATIONS ON PERFORMANCE. . . . .	7
FAN PERFORMANCE SCALING . . . . .	8
SCALING LAWS . . . . .	8
SECONDARY FLOW EFFECTS ON SCALING. . . . .	13
OBSERVATIONS AND RECOMMENDATIONS ON SCALING. . . . .	14
FAN STRUCTURAL LOADS AND DESIGN . . . . .	14
ACKNOWLEDGMENTS . . . . .	18
REFERENCES. . . . .	19

## LIST OF FIGURES

1 - Efficiency and Specific Diameter as Functions of Specific Speed for Three Basic Fan Types . . . . .	21
2 - Variation of Full Scale Fan Efficiency with Model Fan Efficiency for Four Methods of Reynolds Scaling Using an 8-inch Model at 7500 RPM and a 4-foot Full-Scale Fan at 2090 RPM. . . . .	22
3 - Variation of Full Scale Fan Efficiency with Model Fan Efficiency for Two Methods of Reynolds Scaling at Model Speeds of 7000 and 7500 RPM and Full-Scale Speed of 2090 RPM. . . . .	23
4 - Variation of the Efficiency Ratio with the Reynolds Number Ratio for Four Methods of Scaling. . . . .	24
5 - Variation of the Efficiency Ratio with the Reynolds Number Ratio on Log-Log Scale for Four Methods of Scaling . . . . .	25
6 - External Blade Attachment for JEFF (B) Fans. . . . .	26
7 - Representative Fracture Locations and Directions in a JEFF (A) Fan Rotor. . . . .	27

# LIST OF TABLES

	Page
1 - Leading Particulars of JEFF (A) and JEFF (B) Lift Air Supply Systems . . . . .	28
2 - Proposed Fan Designs. . . . .	29
3 - Summary of Reynolds Scaling Equations . . . . .	30
4 - JEFF (A) and JEFF (B) Lift Systems Structural and Mechanical Characteristics. . . . .	31



# NOTATION

D	Fan diameter
D <sub>s</sub>	Specific diameter = $D_T H^{1/4} / Q^{1/2}$
D <sub>T</sub>	Fan rotor disk diameter
H	Fan total head = $\Delta P / \rho g$
HP	Horsepower
K	Ratio of full-scale and model-scale fan efficiencies at maximum efficiency point
k	Constant
L	Lifetime of given structural component
m	Efficiency ratio $\frac{1 - \eta_{FS}}{1 - \eta_{MS}}$
N	Fan rotational speed
N <sub>s</sub>	Specific speed = $N Q^{1/2} / H^{3/4}$
n	Number of cycles to failure
$\Delta P$	Fan exit total pressure in psf
Q	Flow rate
Q <sub>i</sub>	Time that structural component will dwell at given stress level
R	Ratio of minimum to maximum alternating stress
R <sub>e</sub>	Reynolds number = $\frac{D U_T}{\nu}$
S	Applied stress
U <sub>i</sub>	Number of cycles of loading
U <sub>T</sub>	Blade tip speed
$\alpha$	Empirical constant
$\eta$	Efficiency
$\hat{\eta}$	Maximum efficiency
$\lambda_R$	Reynolds number ratio $\frac{R_{eFS}}{R_{eMS}}$

Accession For	
NTIS GRA&I	<input checked="" type="checkbox"/>
DTIC TAB	<input type="checkbox"/>
Unannounced	<input type="checkbox"/>
Justification	
By	
Distribution/	
Availability Codes	
Dist	Avail and/or Special
A	



# NOTATION (CONT)

$\nu$	Kinematic viscosity
$\rho_g$	Specific weight of air
$\lambda_{REF}$	Reynolds number ratio $\frac{R_{eREF}}{R_{eMS}}$
$\phi$	Flow coefficient
$\psi$	Pressure coefficient

## SUBSCRIPTS

FS	Full-scale value
MS	Model-scale value
REF	Reference value
ST	Stall

## ABSTRACT

An analysis of the AALC JEFF lift systems and fans from the viewpoints of performance and structural design is performed. A summary of performance data related to the JEFF lift systems is presented, and suggested approaches for JEFF (A) lift fan design, for which these data provided the baseline information, are provided. Published methods of scaling fan performance data from model to full-scale are evaluated. Finally, the structural design characteristics of the JEFF fans are discussed.

## ADMINISTRATIVE INFORMATION

This study was sponsored by the Naval Sea Systems Command under Task Area S 1417, Task 14174 and administered by the Amphibious Assault Landing Craft Program Office, Code 118, Systems Development Department, of the David W. Taylor Naval Ship Research and Development Center, Bethesda, Maryland.

## INTRODUCTION

The function of a lift system of an air cushion vehicle is to maintain a support cushion of air beneath the craft at a pressure sufficient to counterbalance the craft weight and to deliver an air flow rate sufficient to provide a habitable ride quality and minimize drag. The lift system's major components include the lift fans and engines which power them, the fans inlets, the diffuser which receives fan outflow, and the ducting which transports the air to the cushion chamber or plenum. Hence, any attempt to critically examine the performance of a lift system must properly account for the interaction of all system components. The problem faced by the lift fan designer is to develop a fan design which will deliver the desired performance operating with the above mentioned components and within the framework of other vehicle constraints such as space, weight, and cost. In addition, the designer must take into account the environment in which the fans will operate and must insure that the fans will maintain structural integrity for a reasonably long operating life cycle.

Difficulties have arisen in attempting to satisfy all of these criteria in the design of lift fans for a new generation of amphibious assault landing craft. The purpose of this study is to examine the lift system and lift fan performance the Amphibious Assault Landing Craft (AALC) JEFF craft with the objective of

determining fan design suitability from a performance point of view. A number of requirements have been met in accomplishing this goal. These include a careful review of available fan performance information, an examination of the other lift system components for the JEFF craft, an examination of the rationale for selecting a given fan design, a review of model scale data and the scaling procedures used on these data, and a discussion and description of fan structural design criteria and possible failure mechanisms.

This report presents a summary of pertinent lift fan performance data and suggests sources of performance degradation. The report further presents various design options which could better satisfy the design criteria for the JEFF vehicles. Fan performance scaling is discussed and various published methods which are currently used for scaling performance data from model to full-scale conditions are presented and compared. Finally structural design characteristics of the JEFF fans are described, several possible structural failure mechanisms are identified and briefly discussed.

#### LIFT SYSTEM PERFORMANCE ANALYSIS

The first step required in the analysis of the AALC craft lift system and fan performance is the collection and review of technical data from a variety of sources. These data have been summarized and analyzed with the goal of developing guidelines for the development of new lift fans for future designs of air cushion supported craft. The lift air supply information for the JEFF (A) and JEFF (B) craft taken from Reference 1\* is presented in Table 1. The characteristics of the proposed fan designs for the JEFF (A) and the JEFF (B) are summarized in Table 2.

The information in the first columns of Table 2 gives the performance data for the original JEFF (A) fan and the interim fans. Fan rotational speed needed to achieve the design pressure and flow rate for the original fans was quite high, near 2400 RPM. The specific speed ( $N_s = 293$ ) for this design is more characteristic of a mixed flow fan than a pure centrifugal design. The realization contributed to the decision to replace the original JEFF (A) centrifugal fans with mixed flow design. The stall margin represented by the pressure coefficient ratio in Table 2, is relatively low for the original fan at 39%. Initial attempts by Aerojet General Corporation (AGC) (see Stek<sup>2</sup>) to correct this situation by increasing the blade exit angle were essentially unsuccessful. Rotational speed and

\*Reference are listed on Page 19.

the attendant specific speed were lowered as the blade angle was increased. This had the effect of lowering the stall pressure while moving the stall point to a higher rate, and a loss in efficiency was also observed. The resulting fan performance was considered unacceptable and other alternatives were examined.

There is some evidence that the JEFF (A) fan performance is linked to other components of the lift system and to the installation of the fans in the craft itself. An examination of the performance data from tests<sup>3</sup> of a prototype lift fan for the JEFF (A) conducted in 1972 and reviewed again in September 1976 indicated excellent correlation between the performance of the test fan and that of high efficiency backward airfoil (HEBA"B") fan. An important point revealed in this review was the marked degradation of the prototype performance which occurred when a simulated inlet and plenum were installed.

It is not uncommon for centrifugal fans designed for high specific speeds to experience significant losses in the diffuser unless great attention is paid to the diffuser design. This fact has been noted by a number of experimentors, among them D.J. Myles<sup>4</sup>, who showed that diffusion losses dominate as a centrifugal fan specific speed increases.

There is also evidence indicating that losses associated with the geometric characteristics of the lift system in the JEFF (A) vehicle are significant. In general, to minimize such losses, air ducts should have large diameters, bends in those ducts should have generous radii, and 90° turns and sudden enlargements would be avoided. The nature of the loop pericell system (and to some extent the JEFF (B) bag-finger system) is such that many undesirable flow situations exist. Additionally, the flow from the loop to each of the cells involves flow through an orifice which involves a pressure loss. Losses in the ducts are proportional to the flow rate squared and are traditionally measured by a pressure loss coefficient,  $\Delta P/Q^2$ , which can be determined for various elements in an air distribution system. Such losses were determined for the loop-pericell air distribution system and were reported<sup>5</sup> as early as 1973. In this study it was found that the pressure loss coefficients were high for the loop and cells as compared with other components of the air distribution system, particularly in the forward area of the craft. An estimate based upon these loss coefficients and the other operating characteristics of the lift system, i.e., fan performance, indicates that the pressure loss from the fan exit to the cushion plenum could be as high as 80 psf (3830 Pa) at the craft design operating point.

One of the sources of pressure loss in the lift system is flow separation in a number of lift system components. The test data examined in the process of summarizing the information on proposed fan designs used to construct Table 2 suggest that this may, indeed, be a problem in the inlet of the present designs. It may also be a problem in other regions in the immediate vicinity of the fan rotor and on the elements of the rotor itself. These regions might include the impeller, the fan blades themselves, particularly near their roots along the shroud, the walls of the volute in the transition section between the volute and diffuser, and in the diffuser itself. Other losses which should be considered are blade interference losses, losses due to non-uniform loading on the fan blades (which is affected by the geometry of the gap between the inlet and the rotor), and losses associated with blade profile drag.

The data in Table 2 show that the interim fan for the JEFF (A) does not satisfy the original performance requirements and operates at low efficiency. Its riveted construction and lower operating speed (by approximately 400 RPM) when compared with its predecessor insures its structural survival.

Use of the Westinghouse 66-50 centrifugal design for the JEFF (A) would not be appropriate. While it will satisfy the performance requirements of the lift system, it is very heavy and structural reinforcement of the craft might be required for installation. In addition, the use of steel for a marine environment may considerably increase the maintenance and service requirements associated with the lift system.

The Westinghouse CVL-48 axial flow fan might have satisfied the lift system performance requirement had the JEFF (A) been designed to accommodate it. Very little data are available on this fan and its performance was not included in Table 2. It, like other axial flow machines, suffers severe performance degradation when the uniformity of the air flow delivered to it is poor, as very well might be the case in normal AALC operation. Serious consideration of the fan requires additional study since its installation within the present vehicle constraints would seriously degrade its efficiency.

JEFF (B) fan performance information presented in Table 2 was not examined in great detail in this study. The JEFF (B) fan design is derived from the established performance of the HEBA"B" fan series and supplies air to the craft's bow thrusters as well as to the lift system. Characteristics of the JEFF (B) lift system differ significantly from those of the JEFF (A) giving rise to different sources of flow

losses. Test stand results indicate that the JEFF (B) fan is less efficient than the original JEFF (A) fan or the mixed flow replacement. Operationally, the JEFF (B) fans have performed satisfactorily while undergoing Navy trials, with one repair of the fan blades required due to erosion problems.

#### JEFF (A) FAN PERFORMANCE

##### DESIGN REQUIREMENTS

Available lift system and fan performance data suggest that the fan design for the JEFF (A) should be examined from the viewpoint of the design requirements. These requirements include the following for the AALC JEFF (A) first, the total lift system flow rate is 12800 cfs ( $362 \text{ m}^3/\text{ft}$ ) which must be delivered by 8-four foot (1.22 m) diameter, D, fans; second, the same inlet diffuser and ducting system are retained with their present losses and hence the above stated flow rate has to be delivered at a fan exit total pressure of 171 psf (8187 Pa) subject to a power limitation of 770 hp (0.57 MW) per fan; and third, the vehicle compartment constraints are retained such that the rotor must fit within the original volute.

The remaining critical parameter is the fan rotation speed. The choice in this case is based upon a standard fan design practice of avoiding critical rotational speeds which produce resonant conditions. Such a condition does exist for this fan<sup>6</sup> at a rotational speed of 2750 rpm. Normal design practice is to design for a rotational speed which does not exceed 80% of the critical speed.

Hence, in this case, the design speed should be less than or equal to 2200 RPM.

If the constraints of the previous paragraph and the rotor speed mentioned above are used to compute a traditional specific speed and specific diameter, the results are:

- (1) fan total head:  $H = 2235 \text{ ft (681 m)}$
- (2) specific speed:  $N_s = 271$
- (3) specific diameter:  $D_s = 0.69$

The JEFF (A) design operating point is shown in Figure 1. The curve shows the relation between  $N_s$  and  $D_s$  for maximum rotor efficiency. Although there are no hard limits on  $N_s$  for choosing centrifugal, mixed flow, or axial type fans the requirements of the JEFF (A) may be better satisfied with a mixed flow fan<sup>7</sup> than with a centrifugal fan.

Two other points are particularly noteworthy. First, if the performance of the original Aerojet design with a discharge of 1600 cfs ( $45.3 \text{ m}^3/\text{sec}$ ) per fan and a rotational speed of 2450 rpm were used in the above computation the resulting specific speed would have been 304 suggesting just as strongly the choice of a mixed flow design.

Second, the 8 in (0.203 m) model of the mixed flow fan design proposed by Aerojet Liquid Rocket Company<sup>7</sup> (ALRC) (the only mixed flow design considered thus far) indicates the the performance of this design is best for satisfying the design requirements for the JEFF (A).

#### APPROACHES TO A NEW DESIGN

If the solution to the problem of satisfying the JEFF (A) lift system requirements is restricted to a solution which can alter only the fan rotor and its operation then there are still a number of possibilities which can be explored. It has been suggested that the source of the present poor lift system performance might be associated with flow separation throughout the lift system (i.e., in the inlet and diffuser) and in the fan themselves. Although the original JEFF (A) fan efficiency is relatively high (based upon model data<sup>8</sup>), Figure 1 indicates that some increase in efficiency is possible. Changes in rotor design can lead to increased performance and efficiency. The first possibility involves the concept of blade twist. Flow over the blades can be degraded by a spanwise velocity gradient at the leading edge of the blades. The primary effects of such a gradient are lower total fan efficiency and generally poor fan performance. One way to counteract such an effect is to accomodate it by building twist into the blade sections. The twisted blade, formed before fan assembly, can then be welded or riveted into place on the fan disk.

This technique was used successfully in the design of high performance radial flow fans in the early 1960's.<sup>9</sup> Its incorporation resulted in an extension of the specific speeds of radial flow fans into a much higher regime and produced much higher total efficiencies. Based upon the specific speed calculations made above, it appears that by using blade twist it might be able to extend the performance degradation.

A second proposal involves a reduction in the thickness of the fan blades. Separation of the flow on the fan blades can be caused by the thickness of the profile used for the blades. The airfoil used on the original JEFF (A) rotor was a NACA 6413 airfoil (i.e., a 6% parabolic camber line with the point of maximum camber 40% back from the leading edge of the blade and a 13% thickness ratio). The boundary layer on a blade this thick will be subjected to a severe adverse pressure gradient and could separate well upstream from the trailing edge. Reducing the thickness of the blade will tend to delay the onset of flow separation from the foil. For the same camber the lift will be effectively unchanged but there



will be a noticeable reduction in blade drag and a corresponding increase in lift-to-drag ratio. This should be directly reflected in lower lift engine power requirements.

At lower speeds the performance will be degraded by this approach. In compensation, a slightly higher camber line might be used or a more blunt leading edge might be incorporated to provide a lift improvement. Since the location of the maximum camber point determines the location of the peak minimum pressure point on the blade, moving that point rearward will serve to shift the point where the boundary layer on the foil must first negotiate an adverse pressure gradient closer to the trailing edge of the blade. This will also tend to delay flow separation.

A third approach which is currently being used to overcome flow separation problems associated with strong adverse pressure gradients involves the use of "supercritical" airfoils. These foils were developed at NASA<sup>10</sup> with the intent of reducing the onset of transonic drag rise associated with the flow separation on the airfoil due to a severe adverse pressure gradient (in this case, shock wave induced). Although the supercritical airfoil was developed for use in the transonic regime it has been found to have excellent performance characteristics in subsonic applications.

Supercritical foils are quite thick relative to other transonic foils and are designed with the blade camber concentrated near the trailing edge. Because of this, the upper surface adverse pressure gradient is weak and separation occurs far back on the foil, near the trailing edge. Hence, a possible solution to the flow separation problem in the rotor might be the use of this type blade section if it can be designed to satisfy pressure, flow rate, and efficiency performance requirements. No unusual problems should be encountered in fabricating these blades or in welding or riveting them to the rotor disk.

#### OBSERVATIONS AND RECOMMENDATIONS ON PERFORMANCE

The present study of the JEFF vehicle lift system and lift fan performance indicates that Aerojet's efforts to satisfy the JEFF (A) lift system performance requirements within the present craft constraints with a pure centrifugal fan would meet with some difficulties. Their efforts along the lines of a mixed flow fan appear to be in the proper direction in order to resolve these difficulties. The following requirements would appear to be appropriate. Initiate a program to examine methods by which pressure losses throughout the lift system might be reduced.

Any reduction in system pressure loss will enable the fans to operate at lower exit total pressures and hence at higher discharges. At the same time investigate whether flow separation is a major problem in the lift system. If these tests show that separation problems do exist, consider redesigning both the inlet and the diffuser to overcome them. If separation is present on the fan rotor blades, investigate the changes in fan rotor design suggested in the previous section.

#### FAN PERFORMANCE SCALING

The final criterion for a successful fan design is the satisfaction of the design requirements for a particular application. The construction, operation and testing of full-scale fans is a costly way of arriving at a good design. A better method is to predict fan performance based upon model-scale experiments which are relatively inexpensive to conduct when compared with equivalent full-scale tests. However, the relative flow conditions in fans vary with scale and the designer must consider the scaling laws to obtain full-scale predictions from the model tests.

Empirical scaling laws are used in an attempt to account for the differences in flow conditions between full and model-scale fans arising from the potential and viscous nature of the flow through the fans. Empirical scaling methods are based upon the assumption that the model and full scale flow fields are aerodynamically similar. There are, however, viscous flow effects that complicate this problem. Such effects arise from the possibilities of flow separation, clearances between the fan components, and unsteady flow over the components.

Flow separation is one of the more difficult phenomena to scale since it is associated with adverse pressure gradients in the boundary layer of the flow over the fan components. These effects can only be accounted for through detailed study of boundary layer growth. Theoretical studies of flow separation in fans are still inadequate, and most of the methods for treating this phenomena are of an empirical nature.

#### SCALING LAWS

Fan performance losses associated with viscous drag are a function of Reynolds number. The dependence upon Reynolds number is high when the boundary layer on the surface of the components is laminar or the Reynolds number is low, while the dependence on Reynolds number is low when the flow is turbulent in the high Reynolds number range. Various methods to express performance losses as a function of

Reynolds number have been reviewed in the literature, all of which assume that the flow is fully turbulent. This assumption is justified by the large Reynolds numbers involved in fan scaling. All of these methods account for modifications to the fan efficiency due to the effects of viscosity. A discussion of the development of scaling laws currently in use today and ways for improving the methods is given in the following paragraphs.

Scaling laws currently in use today are based on the assumption of a Reynolds number dependent relationship between model and full-scale performance in which a constant of proportionality is obtained from the losses associated with Reynolds dependent phenomena. Empirical observation (see Stek<sup>11</sup>) has yielded the following relationship between model-scale and full-scale losses

$$(1 - \hat{\eta}_{FS}) = f(Re)(1 - \hat{\eta}_{MS}) \quad (1)$$

where  $\hat{\eta}_{FS}$  and  $\hat{\eta}_{MS}$  are measured at the maximum efficiency point. An assumption is then made relating model-scale to full-scale efficiencies at any point on the curve by a constant.

$$\frac{\eta_{FS}(\phi)}{\eta_{MS}(\phi)} = \frac{\hat{\eta}_{FS}}{\hat{\eta}_{MS}} \equiv K$$

Further, the pressure coefficient is assumed to scale by this same constant

$$\frac{\psi_{FS}(\phi)}{\psi_{MS}(\phi)} = \frac{\eta_{FS}(\phi)}{\eta_{MS}(\phi)} = K$$

Equation (1) can be rearranged as follows

$$\frac{1 - \hat{\eta}_{FS}}{1 - \hat{\eta}_{MS}} = f(Re)$$

$$\frac{\frac{1}{\hat{\eta}_{MS}} - K}{\frac{1}{\hat{\eta}_{MS}} - 1} = f(Re)$$

Solving for K results in

$$K = \frac{1}{\eta_{MS}} (1 - f(R_e)) + f(R_e) \quad (3)$$

For  $f(R_e) = 1$  the potential flow case is obtained when  $K = 1$ . Potential flow theory implies that the non-viscous flow patterns around geometrically similar bodies are modified by the same geometric ratio as that of the bodies. The pressure and velocity fields are also modified by this ratio and consequently the efficiencies of the model-scale fan and the full-scale fan are equal.

In the absence of empirical data the function of Reynolds number may be assumed to be a constant

$$f(R_e) = k$$

Equation (3) now reduces to

$$K = \frac{1}{\eta_{MS}} (1 - k) + k$$

Experimental investigations have suggested that

$$f(R_e) = \lambda^\alpha \quad (4)$$

where  $\lambda = \lambda_R = \frac{R_{eFS}}{R_{eMS}}$  or  $\lambda = \lambda_{REF} = \frac{R_{eREF}}{R_{eMS}}$

The two Reynolds number ratios arise from the fact that some investigators use a reference Reynolds number rather than full-scale Reynolds number. The value of  $\alpha$  is determined experimentally.

A more general form of the scaling laws is to assume that the efficiency ratio is not constant, but it is allowed to vary with flow rate.

$$\frac{\eta_{FS}}{\eta_{MS}} = \psi_1(\phi)$$

Now the nondimensional pressure is given by

$$\frac{\psi_{FS}}{\psi_{MS}} = \psi_1(\phi)$$

The next step is to allow the efficiency ratio and the pressure ratio to be independent functions of  $\phi$

$$\frac{\eta_{FS}}{\eta_{MS}} = \psi_1(\phi)$$

$$\frac{\psi_{FS}}{\psi_{MS}} = \psi_2(\phi)$$

Formulating scaling laws as suggested above should improve full-scale performance predictions and an experimental investigation program would be needed to determine the functional relationships.

Several empirical scaling methods have been published in the form of Equation (2), where  $f(R_e)$  is given by Equation (4). The most noteworthy of these methods are the following:

1. Aerojet<sup>11</sup>

$$f(R_e) = (\lambda_{REF})^{-0.116}$$

(based upon 3KSES model fan test data).

2. Bell Aerospace<sup>12</sup>

$$f(R_e) = (\lambda_R)^{-0.114}$$

3. R.C. Pamreen<sup>13</sup>

$$f(R_e) = (\lambda_{REF})^{-0.164}$$

4. Ackeret<sup>14</sup>

$$f(R_e) = 0.5 + 0.5(\lambda_R)^{0.2}$$

## 5. NASA<sup>15</sup>

$$f(R_e) = (\lambda_R)^{-0.2}$$

The Reynolds scaling equations are summarized in Table 3. The relative difference between the methods can be seen in Figure 2 which shows the variation of full-scale fan efficiencies with model-scale fan efficiencies for a particular pair of Reynolds numbers. All models are shown with a model fan of 8 in (0.203 m) diameter at 7500 RPM and a full-scale fan of 4 ft (1.219 m) diameter at 2090 RPM.

Figure 3 shows the variation of full-scale fan efficiency with model fan efficiency for model speeds of 7000 and 7500 RPM, using Aerojet's and Ackeret's equations. This difference is less than 1% but this can be important from the view of full-scale performance predictions. A one percent difference in loss ratio could result in a 6% difference in pressure requirements as indicated in Figure 4.

Figure 4 shows the variation of the loss ratio with the Reynolds number ratio  $\lambda_R$  for each method. The curves are developed for use with the maximum model-scale efficiency. In Figure 5, which shows the same results in a log-log representation, the Ackeret method is seen to deviate from a straight line. Also indicated in Figures 4 and 5 are some empirical values taken from the NASA<sup>15</sup> report. These values were found by varying the rotational speed of a 6 inch radial bladed centrifugal compressor. The data points cover only a small range but do indicate the accuracy that these methods would give in that situation.

As already indicated, the previously described methods assume that the flow is fully turbulent. An attempt to relax this assumption has been presented by Rotzoll<sup>16</sup>. The relationship can be expressed as

$$\frac{1 - \eta_{FS}}{1 - \eta_{MS}} = \lambda_R^\alpha$$

where  $\alpha$ , the exponent, is allowed to vary with Reynolds number and specific fan speed. The variation of  $\alpha$  with Reynolds number appears to be an attempt to account for laminar and turbulent flow losses using the same equation. Direct comparison of this method with the previous methods was not possible due to unavailability of experimental data from which coefficients could be derived. The method may have merit if enough experimental data are available to determine

the variation of the proportionality coefficient,  $k$ , and the scaling exponent,  $\alpha$ .

#### SECONDARY FLOW EFFECTS ON SCALING

Secondary flow phenomenon are characterized by unsteady fluid motion or by fluid motion in directions contrary to that of the main flow. These flows have two effects: first, they provide a velocity disturbance in the main stream and second, they effect a transfer of momentum from one part of the flow to another. Mechanisms of these flows are only imperfectly understood and their Reynolds number dependence is not known; therefore, their effects on scaling are not understood. Since secondary flows in this situation result from boundary layers formed from essentially 2-D flow, any factors that increase the boundary layer thickness should also increase the intensity of the secondary flow. Thus, the losses resulting from the disturbances to the main flow increase as the boundary layer grows. Moreover, by moving low energy material from one area to another, secondary flows can modify the transition from turbulence to separation.

The phenomenon of flow separation in centrifugal fans is associated with the development of adverse boundary layer pressure gradients. Transverse pressure gradients may appear whenever there is curvilinear relative motion between the main flow and its boundaries. Any curved flow or rotating blades may thus produce pressure gradients that are perpendicular to the direction of the main flow. When the motion of the main flow adjusts itself to be in equilibrium with these gradients, the boundary layers are subjected to acceleration in a direction perpendicular to the main flow. The result is a secondary flow which may lead to flow separation.

The effects described above are associated with adverse pressure gradients. If the pressure gradients are favorable, i.e., the fluid is accelerated in the direction of its main stream motion, then the establishment of secondary flows will be suppressed. A good fan design should take this into account and should attempt to establish favorable pressure gradients in the boundary layer. As a general rule, if the ratio of the fluid velocity at the leading and trailing edges of the fan blades is larger than or equal to 2, the boundary layer is deemed to be separated. The losses associated with separating flows are not Reynolds number dependent and have to be investigated separately.

Another secondary flow phenomenon that needs further investigation is that associated with the dimension and shape of clearances between the various fan components. Their effect is to instigate secondary eddying flows between the components that are in relative motion. These eddying flows interfere with the

mean flow and thus produce additional losses in fan performance. Losses can increase as the clearance between the fan components increases. Clearance effects are more pronounced on model-scale fans where the ratio of clearance to chord length is larger than in full-scale fans. These effects are not accounted for in the previous method of scaling and may provide a reason for the disagreement noted in Figures 4 and 5, particularly as  $\lambda_R$  increases.

Other sources of losses not described by the above methods are those associated with unsteady components of the flow. Unsteady effects appear in the form of pressure fluctuations above or below the design levels. Their main influence seems to be on the transition points from laminar to turbulent flow. The exact mechanism through which unsteady effects influence losses in performance is not known. This is an area which warrants further research.

#### OBSERVATIONS AND RECOMMENDATIONS ON SCALING

The previously described methods for scaling of fan performance provide some level of accuracy under the assumption of fully turbulent flow and absence of separation. However, the difference in the various methods as well as the scatter in the experimental data from which these scaling equations were derived indicate the presence of secondary effects which should be investigated for a more complete understanding of the problem.

In general the scaling equations use the rotor tip speed in the definition of the respective Reynolds numbers. The Reynolds number should represent properties of the air flow around the fan blades and not the fan itself, and therefore the velocity of the flow relative to the blade should be used in calculating the Reynolds number. For axial flow fans the difference between the relative flow velocity and the rotor tip speed seems to be small and hence the use of the latter velocity for the determination of the Reynolds number seems justifiable. In centrifugal fans, however, where the angle at which the flow leaves the fan blades may be quite high, the difference between the two velocities may be appreciable and the relative velocity should be used in the future to define Reynolds number.

#### FAN STRUCTURAL LOADS AND DESIGN

The structural design of lift fans for an air cushion vehicle involves detailed knowledge of the structural loads, the mechanical properties of the material, and the effects of fabrication technique. Loads exerted on the fan structure (shrouds, blades, and backplate) are determined by the superposition of the steady and



unsteady aerodynamic loads and the centrifugal loads. The magnitude, direction, and distribution of the loads over the fan structure must be determined before an accurate structural evaluation can be made. Strength and fatigue properties of the selected material must be known to define structural integrity and the expected life of the fan. Consideration must then be given to how the fan components will be assembled and how the fabrication technique changes material properties or creates stress concentrations. These topics are discussed in general and with specific reference to the JEFF craft.

The method employed to attach the various structural components of the fan together so that they form a rigid structure is different for the JEFF (A) and (B) fans. The JEFF (B) blades are constructed using aluminum 6061-T6 for the top and bottom skins, while the leading edge is constructed of stainless steel. The backplate is bolted to a flange on the shaft and the blades are attached to the backplate by external angles as shown in Figure 6<sup>17</sup>. On the other hand, the original JEFF (A) fan and its mixed flow replacement are both of welded construction. The blades were attached to the backplate with electron beam (EB) T-joint welds as shown in Figure 7<sup>18</sup> for the original fan design. The shroud assembly consisted of three rings which were also EB welded. Further details on the material used and method of construction for the JEFF craft are shown in Table 4.

#### FAN STRUCTURAL LOADS

Loads exerted on fans are of three basic types. The most important are the centrifugal loads which are generated by rotating the fan structural members about the fan axis, the center of gravity of these members being located at a distance away from that axis. Second are the aerodynamic loads which are associated with the development of lift, including any unsteady loading due to stall. Third are the gyroscopic loads which are associated with the rotation of the structural members of the fan in a plane normal to the plane of rotation. Such loads are commonly generated when the craft is pitching or rolling. If the fan is considered in isolation then the two types of loading important in the design are the centrifugal and aerodynamic loads.

In the steady state operation of a centrifugal fan, the rotation induced loads constitute the main source of fan loading. If it is assumed that the centrifugal loading is distributed along the chord of the profile, a higher concentration of loading will exist in the region extending from the leading edge of the profile to the quarter-chord point due to higher concentration of blade mass in this area.

The shearing forces and moments developed at the attachments of the blades with the shroud and the backplate will be higher around the region described. Since the shroud and backplate have finite thickness and cannot be assumed to behave as thin membranes, these shearing forces give rise to considerable bending moments and bending stresses at the attachments of these surfaces with the blades. These considerations coupled with the fact that there is a sharp discontinuity of the surface at the attachment, leading to stress concentrations in the region, indicate that the region from the leading edge to the blade quarter-chord is subjected to high stresses which may lead to blade attachment and structural failure.

Aerodynamic loads arise mainly from the flow of air around the fan blades. The blade sections are of the airfoil type and as such produce lift forces which contribute to the loading on the blade, the blade attachments and consequently on the shroud and backplate themselves. Lift force is a function of the velocity of air inflow, blade rotational speed, the angle of attack and the shape of the section. Since the fan blades are usually of constant cross-section, i.e., no taper, the lift developed can be determined from 2-D airfoil theory, corrected for finite aspect ratio effects using Prandtl's finite aspect ratio formula.<sup>19</sup> The resulting lift coefficient must be corrected for cascade effects and the effects of viscosity. Cascade effects can be accounted for using standard procedures such as Weinig's<sup>20</sup> theory, while viscosity can be taken into account using experimental results.

In the preliminary stages of the design the lift force can be assumed to be applied at the quarter-chord point of the blade section. It is clear that structure welds coinciding with or in the vicinity of this point are subjected to maximum loading forces which can lead to weld fractures. It is shown on Figure 7 that the welds on the shroud surface of the original JEFF (A) fans lie in the vicinity of the quarter-chord point of the blade section. It is also noted in Figure 7 that fatigue cracks developed in these shroud welds on both the suction and pressure sides of the blades at this quarter-chord point. At the blade/shroud pressure side the fatigue cracks (SP) began in the shroud at the fillet weld root intersection with the shroud outer circumferential EB weld and extended into and through the shroud. At the blade/shroud suction side the cracks (SS1) began in the blade outer surface at the edge of the fillet weld and extended inward through the blade. Further, at the blade/shroud suction side the cracks (SS2) began in the fillet weld root and extended outward through the center of the fillet weld. All of these

cracks have in common a location in the vicinity of the quarter-chord point where the total aerodynamic loading is assumed to be applied. No cracks developed in the outer EB duct welding passing near the trailing edge of the blade section where the aerodynamic loading is small. On the basis of the geometry of the blade cross-section shown in Figure 7, the SS2 crack development may be associated with both the quarter-chord point loading and also the high suction pressure value in this area. The cracks that developed in the blade leading edge in both the shroud (SLE) and backplate (BLE) locations are probably due to the high pressure loading at the leading edge region which is common to all usual airfoil type sections.

In the detailed stage of the design, calculation of the pressure distribution on both the pressure and suction sides of the blades, corrected for compressibility, provides a picture of the load distribution on the blade sections in the chordwise direction. This indicates the loads exerted on the welds along the attachments of the blade to the shroud or backplate. Particular attention should be paid to the weld in the vicinity of the leading edge of the blades where the pressure distribution, particularly on the suction side, is characterized by large values. Weld depth and reinforcement of the attachment in the leading edge region must be seriously considered. A detailed pressure distribution also indicates areas where separation and reattachment, which is a source of vibratory loading, may occur.

Vibratory loads can be induced upon the blades, shroud, and backplate of a fan due to variations in aerodynamic loading or pressure fluctuations in the fan. Cyclic aerodynamic loading of a fan may have several sources one of which arises from operating the fan at different conditions associated with changes in RPM and inflow velocity. A second source may be produced by separation and reattachment of the flow at a constant RPM. If separation leads to stalling of the blades, then variation in lift loading can be considerable. Another source of periodic pressure fluctuations occurs as a centrifugal fan blade passes from the volute exit lip, where static pressure is a maximum to the scroll minimum circumference where the static pressure is a minimum. Since pressure fluctuation can occur with every rotor revolution, the cyclic loading of the structure may be a serious cause of fatigue. If the frequency of these aerodynamic vibratory loads coincides with a natural frequency of the fan blade or fan structure, resonance occurs, leading to a magnification of the stresses in the fan structure. Although aerodynamic loads in centrifugal loading, their oscillatory behavior superimposed on high mean centrifugal loads may have significant detrimental effects on the structural performance

due to fatigue.

If the results of the investigations mentioned above indicate that the fan structure is subjected to resonant loading for extensive operating times, then the fan design should be altered. If axial fans are to be employed, the fluctuating aerodynamic loads, which will be much higher than the corresponding loads on centrifugal fans, have to be estimated and the fan design has to be judged by the same considerations. For axial fans it is particularly important that the air inflow to the blades be as uniform as possible for minimum vibration excitations. If high fluctuating loads are observed, then the inlet of the fan has to be altered to achieve a more uniform air inflow to the fan blades.

#### ACKNOWLEDGMENTS

The initial data analysis and preparation were performed in the High Performance Craft Dynamics Branch by L. Murray. The fan performance comparison was developed by T. Waters as data were made available. Portions of the analysis were performed by J. Schneider and N. Caracostas with the assistance of M.V. Bullock of ORI, Inc. The authors are extremely grateful to each of these individuals for their contribution to this summary document.

#### REFERENCES

1. Amphibious Assault Landing Craft Technology Baton A6.1, "Lift Air Supply Systems," (May 1980).
2. Stek, J.B., "JEFF (A) Scale-Model Lift Fan Test Program Redesigned Rotor Performance Validation," Aerojet-General Corp. Report ALRC 9700-0681 (July 1977).
3. Tangren, R.F., "Performance of the Lift Fan for the JEFF (A) from Tests at the North 30th Street Facility," Aerojet-General Corp. Engineering Note AALC 835-0143 (September 1976).
4. Myles, D.J., "An Analysis of Impeller and Volute Losses in Centrifugal Fans," Proceedings of the Institute of Mechanical Engineers (1969-70).
5. Csaky, T.G., "Performance of the Fan for the JEFF (A), Aerojet-General Corp.," Memorandum to Z.G. Wachnik (February 1973).
6. Communication from Westinghouse Corp. to DTNSRDC (June 23, 1977).
7. Lorenc, S.A., "JEFF (A) Mixed Flow Model Lift Fan Performance Evaluation (8 and 16 blade configuration)," Aerojet Liquid Rocket Company Report CDN 4357 (March 1978).
8. Stek, J.B., "JEFF (A) Scale Model Test Program Lift Fan Performance Evaluation," Aerojet Liquid Rocket Company Report 9737-0621 (April 1977).
9. Eck, B., "Fans," Pergamon Press, Braunschweig (1973).
10. Blackwell, J.A., Jr., and G.A. Pounds, "Wind Tunnel Interference Effects on a Supercritical Airfoil at Transonic Speeds," Lockheed Georgia Report (June 1976).
11. Stek, J.B., "JEFF (A) Scale-Model Test Program Lift Fan Evaluation," Aerojet-General Corp. Report ALRC 9737-0621 (April 1977).
12. Personal communication between D. Moran (DTNSRDC Code 1572) and J. Allison (Bell Aerospace Company).
13. Pampreen, R.C., "Small Turbomachinery Compressors and Fan Aerodynamics," Transactions of the ASME, Journal of Engineering for Power (July 1973).
14. "Test Code for Air Moving Devices," AMCA Standard 210-67.
15. Heidelberg, L.C., C.L. Ball, and C. Weigel, "Effect of Reynolds Number on Overall Performance of a 6-inch Radial-Bladed Centrifugal Compressor," NASA Report TN D-5761 (April 1970).

16. Balje', O.E., "A Study on Design Criteria and Matching of Turbo-machines: Part B - Compressor and Pump Performance and Matching of Turbocomponents," Transactions of the ASME, Journal of Engineering for Power, pp. 103-114 (January 1962).
17. Bell Aerospace Company, "AALC Program Phase II Landing Craft JEFF (B) Monthly Progress Report (August 1972).
18. Stakee, W.A., "JEFF (A) Fan Rotor Failure Analysis," Aerojet-General Corp. Report AALC/56/0156A (August 1977).
19. Abbott, I.H., and A.E. von Doenhoff, Theory of Wing Sections, Dover Publications, New York (1959).
20. Sedov, L.I., Two-Dimensional Problems in Hydrodynamics and Aerodynamics, John Wiley & Sons, Inc., New York (1965).

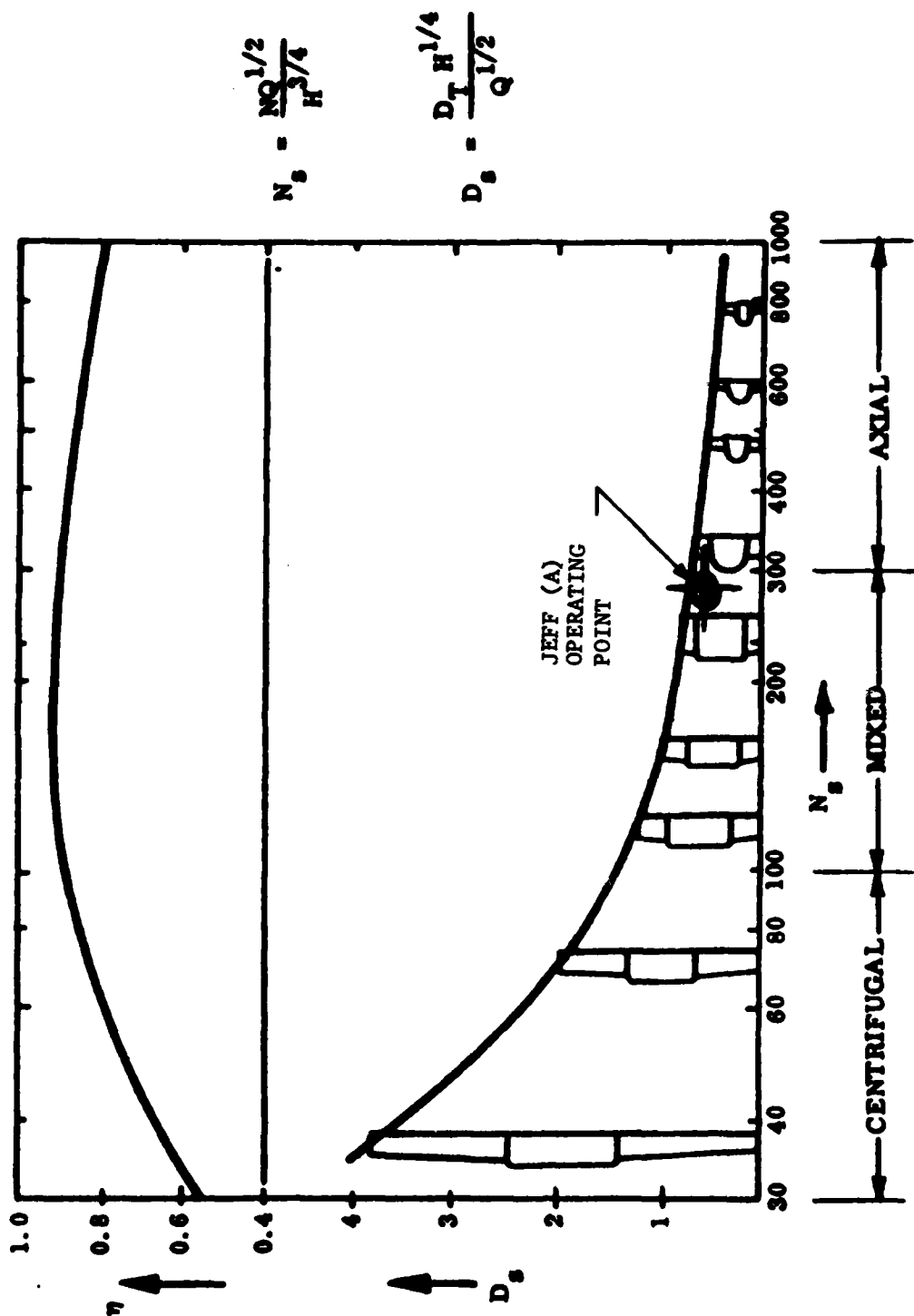


Figure 1 - Efficiency and Specific Diameter as Functions of Specific Speed for Three Basic Fan Types

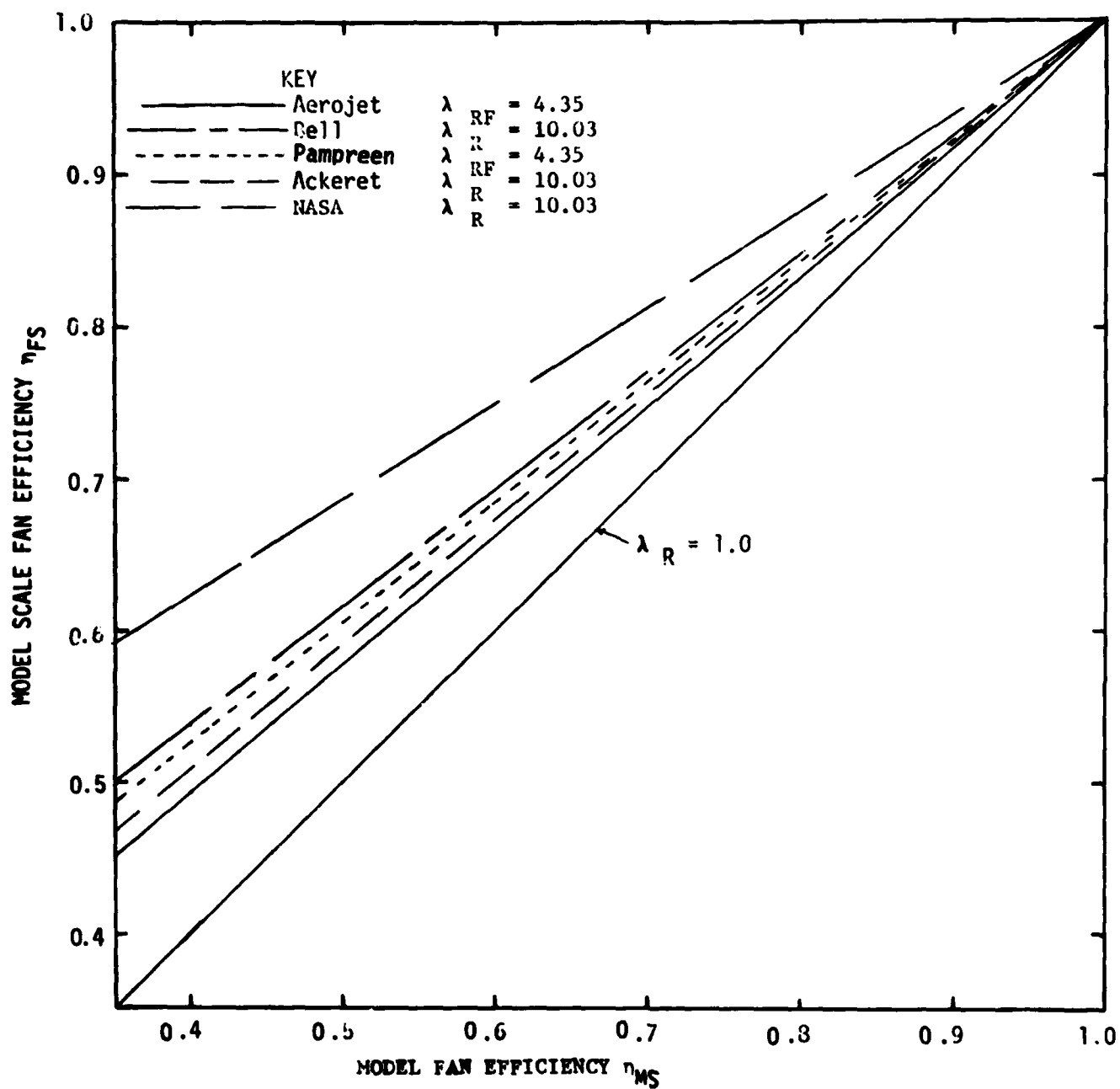


Figure 2 - Variation of Full Scale Fan Efficiency with Model Fan Efficiency for Four Methods of Reynolds Scaling Using an 8-inch Model at 7500 RPM and a 4-foot Full-Scale Fan at 2090 RPM



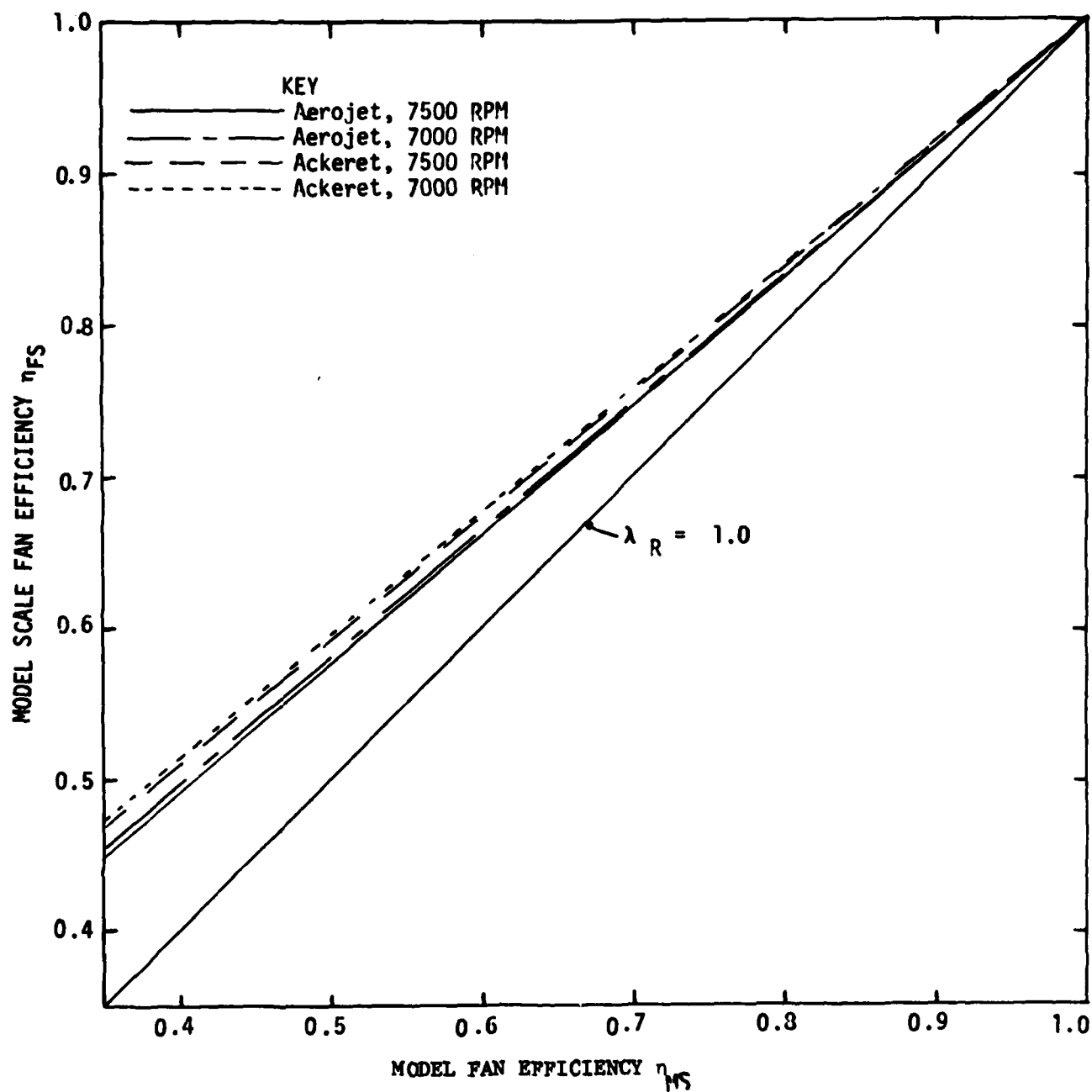


Figure 3 - Variation of Full Scale Fan Efficiency with Model Fan Efficiency for Two Methods of Reynolds Scaling at Model Speeds of 7000 and 7500 RPM and Full-Scale Speed of 2090 RPM

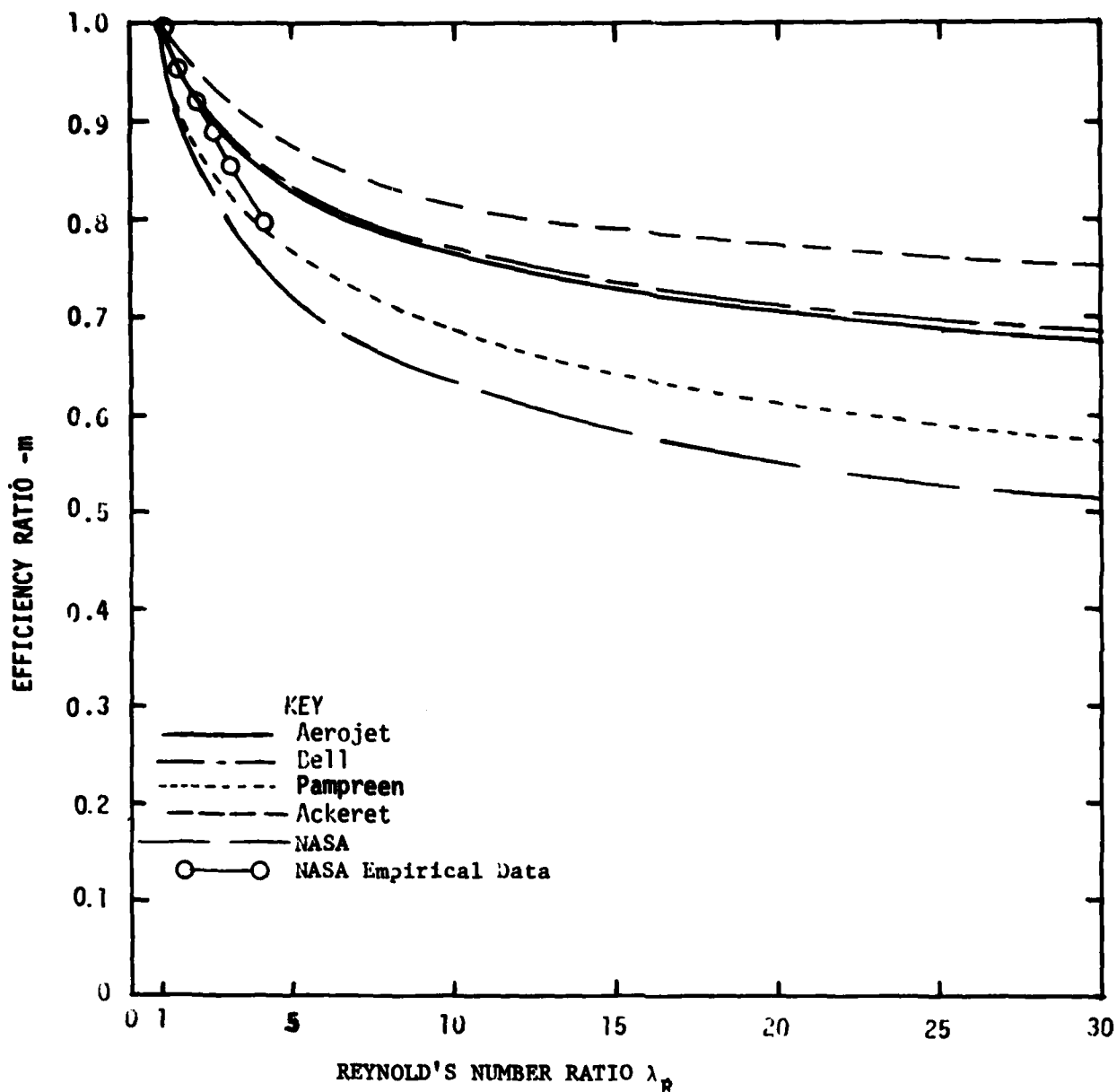


Figure 4 - Variation of the Efficiency Ratio with the Reynolds Number Ratio for Four Methods of Scaling

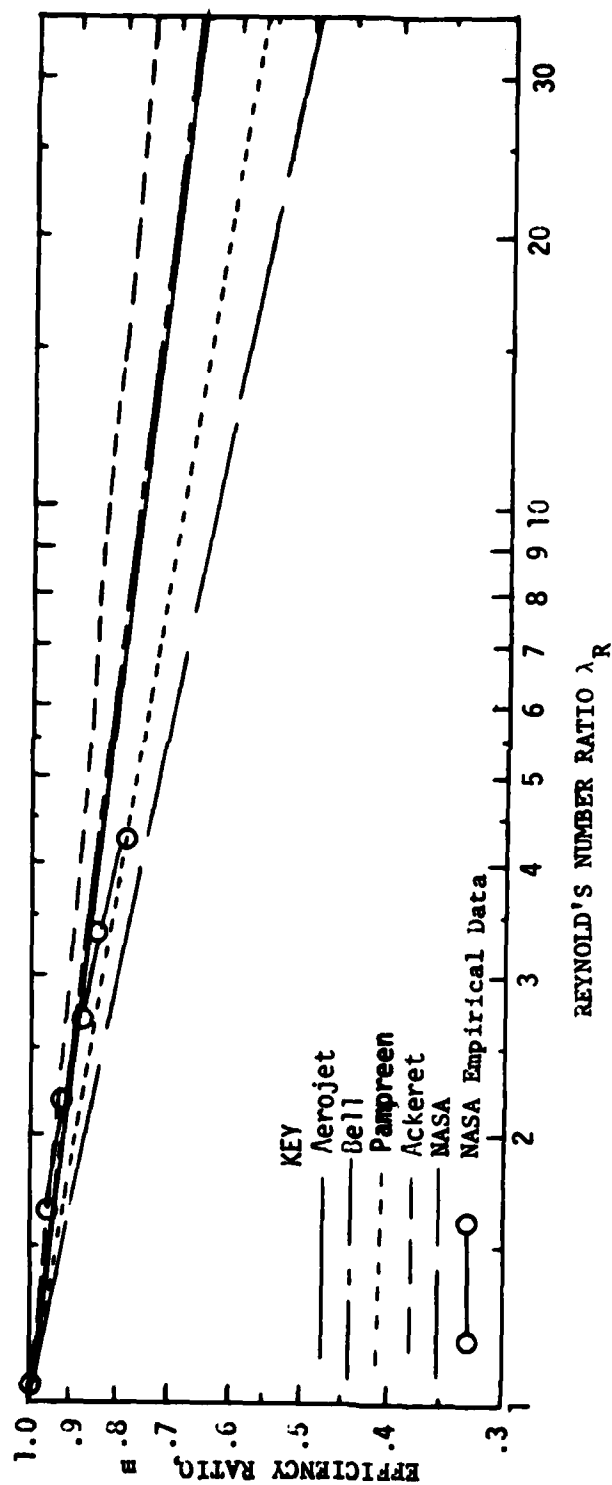


Figure 5 - Variation of the Efficiency Ratio with the Reynolds Number Ratio on Log-Log Scale for Four Methods of Scaling

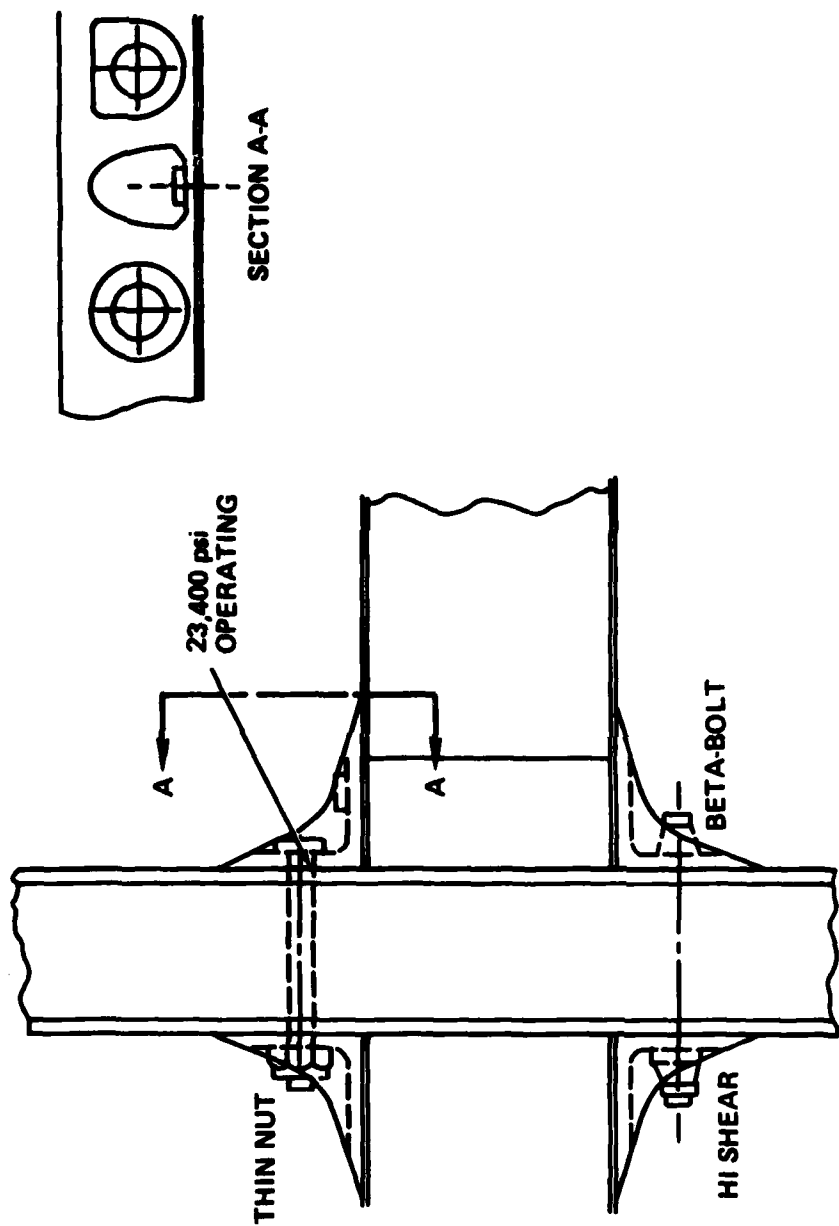


Figure 6 - External Blade Attachment for JEFF(B) Fans

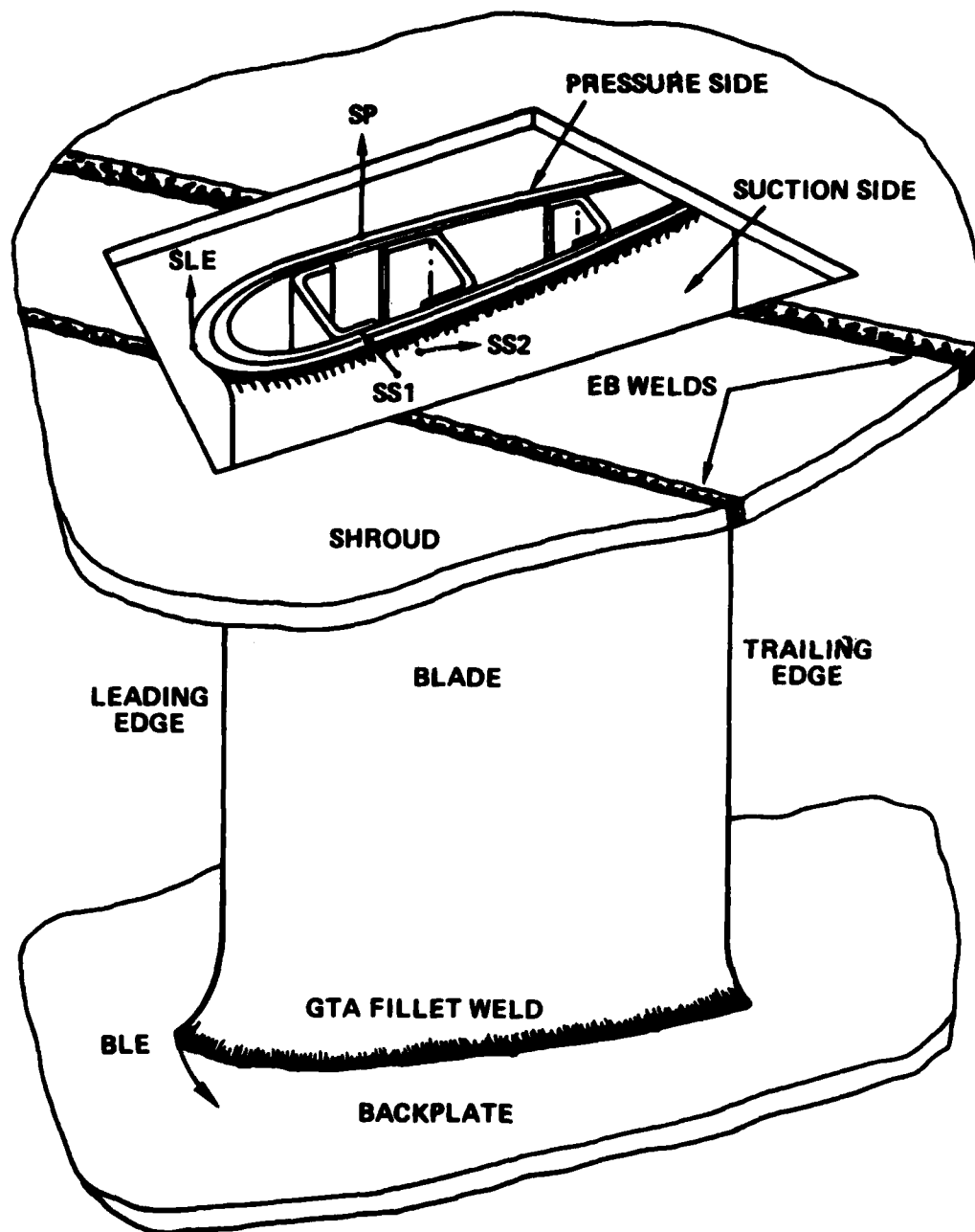


Figure 7 - Representative Fracture Locations and Directions in a JEFF(A) Fan Rotor

**TABLE 1**  
**LEADING PARTICULARS OF JEFF (A) & JEFF (B)**  
**LIFT AIR SUPPLY SYSTEMS**

	UNITS	JEFF(A) <sup>b</sup>	JEFF(A) <sup>c</sup>	JEFF(B)
Type of Fans-----	-	Centrifugal	Centrifugal	Centrifugal
Manufacturer-----	-	Aerosmith	ALRC	Task
Rotor Material-----	-	Aluminum	Aluminum	Aluminum
Type of Construction-----	-	Welded	Riveted	Riveted
Number of Fans per Ship Set-----	-	8	8	8
Volute Volume Ratio-----	-	7.0	5.6	7.0
Rotor Tip Diameter-----	ft(m)	4.0 (1.22)	4.0 (1.22)	5.0 (1.52)
Number of Blades per Rotor-----	-	12	19	12
Blade Exit Width-----	ft(m)	0.935(0.285)	1.17(0.357)	1.077(0.328)
Blade Exit Angle $\beta_2$ -----	Degrees	30	90	61.3
Continuous Rotational Speed*-----	rpm	2410	2090	1750
Rotor Tip Speed*-----	ft/s(m/s)	504 (154)	438 (133.5)	458 (139.6)
Total Air Volume Flow Rate*-----	ft <sup>3</sup> /s(m <sup>3</sup> /s)	12,800(362)	12,800(362)	19,400(546)
Cushion Air Volume Flow Rate*-----	ft <sup>3</sup> /s(m <sup>3</sup> /s)	12,900(362)	12,800(362)	10,400(293)
Average Flow Rate per Fan*-----	ft <sup>3</sup> /s(m <sup>3</sup> /s)	1,600(45.3)	1,600 <sup>d</sup> (45.3)	2,425(68.65)
Cushion Area-----	ft <sup>2</sup> (m <sup>2</sup> )	3,530 (328)	3,530 (328)	3,200 (297)
Loop/Bag Feed Hole Area**-----	ft <sup>2</sup> (m <sup>2</sup> )	19.41(1.803)	9.68(0.899)	8.50(0.790)
Wet Deck Duct Exit Area**-----	ft <sup>2</sup> (m <sup>2</sup> )	16.17(1.50)	16.17(1.50)	24.1(2.23)
Fan Discharge Area**-----	ft <sup>2</sup> (m <sup>2</sup> )	8.31 (0.772)	8.31(0.772)	12.3(1.142)
Total Inlet Area-----	ft <sup>2</sup> (m <sup>2</sup> )	33.13(3.08)	33.13(3.08)	48.67(4.52)
Cushion Pressure*-----	lb/ft <sup>2</sup> (Pa)	93.5(4480)	76(3640)	103.1(4940)
Bag or Loop Pressure*-----	lb/ft <sup>2</sup> (Pa)	114.1(5466)	96.5(4620)	144.3(6916)
Bag/Cushion Pressure Ratio*-----	-	1.22	1.27	1.40
Fan Exit Static Pressure*-----	lb/ft <sup>2</sup> (Pa)	121(5796)	-	158 (7565)
Fan Exit Total Pressure**-----	lb/ft <sup>2</sup> (Pa)	170 (8140)	130 (6720)	170 (8140)
Fan Flow Coef. at Cont. Flow*-----	-	0.270 <sup>b</sup>	0.249	0.313
Fan Head Coef. at Cont. Flow*-----	-	0.303 <sup>b</sup>	0.308	0.336
Fan Specific Speed at BEP-----	-	190 <sup>b</sup>	246.5	239 <sup>a</sup>
Fan Specific Diameter at BEP-----	-	0.894 <sup>b</sup>	0.888	0.740 <sup>a</sup>
Fan Specific Speed at Design*-----	-	281 <sup>b</sup>	298	269 <sup>a</sup>
Fan Specific Diameter at Design*-----	-	0.700 <sup>b</sup>	0.654	0.494 <sup>a</sup>
Fan Total Efficiency at BEP-----	-	0.84 <sup>b</sup>	0.59	0.685 <sup>a</sup>
Fan Static Efficiency at BEP-----	-	0.74 <sup>b</sup>	-	0.64 <sup>a</sup>
Fan Total Efficiency at Design*-----	-	0.71 <sup>b</sup>	0.44	0.67 <sup>a</sup>
Fan Static Efficiency at Design*-----	-	0.51 <sup>b</sup>	-	0.62 <sup>a</sup>
Lift Transmission Gear Ratio-----	-	6.114	6.114	8.548
Shaft Power Per Fan Cont.*-----	hp(kw)	652.5(486)	266(646)	562(420)
Total Continuous Lift Power*-----	hp(kw)	5220(3900)	6925(5168)	4500(3360)
No. & Type of Lift Engines-----	-	2, TF 40	2, TF 40	Inc. TF 40
Continuous Power SFC-----	lb/hp/hr(g/wh)	0.64(0.39)	0.64(0.39)	0.61(0.37)
Hemline Peripheral Length-----	ft(m)	252(76.8)	252(76.8)	24-(76.4)
Mean Hemline Hovergap*-----	ft(m)	0.27(8.2)	-	0.21(6.4)
Total Lift System Efficiency*-----	-	43	25.5	43
Rotating Weight (per Rotor)-----	lb(hg)	130 (59)	224 (97.5)	-
Rotor Moment of Inertia-----	-	156 (70)	-	-
Total Lift Air System Weight-----	LT(t)	10.3(10.3)	10.6(10.77)	-

\* At 330,000 Lb Gross Weight, Continuous Power, 100°F (268,000 lb limit for Interim fans)

† Excludes Stability Trunk Drainage Holes

\*\* Per Fan

LT:- Long Tons;

(t):- Metric Tons;

\* Average

\* Six fans feeding loop on JEFF(A)

Int.- Integrated Lift & Propulsion

- Based on model data, 5.1" diameter without scale corrections.
- Fans for the JEFF(A) have been redesigned (Nov. 1977). Characteristics shown in this column are those predicted for the original configuration.
- Characteristics of the "Interim" design fans which are presently operating (Feb. 1980) in the JEFF(A). The fans are currently being replaced with mixed-flow fans.
- Goal is 1,600 ft<sup>3</sup>/sec (minimum 10,000 ft<sup>3</sup>/sec).

TABLE 2  
PROPOSED FAN DESIGNS

FANS CHARACTERISTICS	ALRC 40.5°	INTERIM FANS	ALRC 60°	ALRC 90°	ALRC MIXED FLOW	WE 66-50	JEFF (B)
Flow Rate, cfs(m <sup>3</sup> /sec)	1600(45.3)	1600(45.3)	1600(45.3)	1600(45.3)	1600(45.3)	1800(51.0)	2425(68.7)
Fan Rotational Rate;rpm	2410	2090	2157	2025	2200	2160	1748
Maximum efficiency	0.84	0.59	0.78	0.65	0.77	0.88	0.68
Design efficiency	0.71	0.44	0.69	0.59	0.72	0.83	0.67
Shut-off pressure,psf (Pa)	214 (10246)	210 (10055)	201 (9624)	190 (9097)	238 (11395)	308 (14747)	NA
$\phi$	0.27	0.249	0.30	0.319	0.312	0.28	0.27
$\psi$	0.303	0.308	0.37	0.425	0.40	0.375	0.313
D <sub>S</sub>	0.686	0.686	0.686	0.686	0.686	0.647	0.672
N <sub>S</sub>	293	258	267	250	257	283	268
$\psi_{ST}/\psi$	1.39	1.61	1.29	1.19	1.42	1.59	NA

All fan designs have the following common characteristics:

Inlet total pressure = 14.7 psia (101342 Pa)  
 Inlet total temperature = 100°F (37.8°C) \*Aeroject Liquid Rocket Company  
 Humidity at Inlet = 50%  
 Required fan exit total pressure = 170 psf (8140 Pa)

TABLE 3  
SUMMARY OF REYNOLDS SCALING EQUATIONS

Potential	$\frac{1 - \eta_{FS}}{1 - \eta_{MS}} = k \left( \frac{R_{eFS}}{R_{eMS}} \right)^0$
Aerojet	$\frac{1 - \eta_{FS}}{1 - \eta_{MS}} = \left( \frac{R_{eREF}}{R_{eMS}} \right)^{-0.116}$
Bell	$\frac{1 - \eta_{FS}}{1 - \eta_{MS}} = \left( \frac{R_{eFS}}{R_{eMS}} \right)^{-0.114}$
Pampreen	$\frac{1 - \eta_{FS}}{1 - \eta_{MS}} = \left( \frac{R_{eREF}}{R_{eMS}} \right)^{-0.164}$
Ackeret	$\frac{1 - \eta_{FS}}{1 - \eta_{MS}} = 0.5 + 0.5 \left( \frac{R_{eFS}}{R_{eMS}} \right)^{-0.2}$
NASA	$\frac{1 - \eta_{FS}}{1 - \eta_{MS}} = \left( \frac{R_{eFS}}{R_{eMS}} \right)^{-0.2}$
Rotzoll	$\frac{1 - \eta_{FS}}{1 - \eta_{MS}} = \left( \frac{R_{eFS}}{R_{eMS}} \right)^c$
	$R_{eREF} = 4 \times 10^6$



TABLE 4  
JEFF(A) AND JEFF(B) LIFT SYSTEM STRUCTURAL  
AND MECHANICAL CHARACTERISTICS

ELEMENT	MATERIAL		METHOD OF CONSTRUCTION	
	JEFF(A)	JEFF(B)	JEFF(A)	JEFF(B)
Inlets	Fiberglass with polyurethane coating	Fiberglass	Cast and milled	Cast
Impellers	Aluminum	Aluminum with honeycomb blades	Electron beam welding	Bolt
Volutes	Aluminum plate	-	Weld	Integral part of structure
Exit Ducts	Aluminum alloy	-	Integral part of structure	Riveted
Blades	Aluminum alloy	End grain balsa core and .052" aluminum skins	Cast and Milled	Epoxy

#### **DTNSRDC ISSUES THREE TYPES OF REPORTS**

- 1. DTNSRDC REPORTS, A FORMAL SERIES, CONTAIN INFORMATION OF PERMANENT TECHNICAL VALUE. THEY CARRY A CONSECUTIVE NUMERICAL IDENTIFICATION REGARDLESS OF THEIR CLASSIFICATION OR THE ORIGINATING DEPARTMENT.**
- 2. DEPARTMENTAL REPORTS, A SEMIFORMAL SERIES, CONTAIN INFORMATION OF A PRELIMINARY, TEMPORARY, OR PROPRIETARY NATURE OR OF LIMITED INTEREST OR SIGNIFICANCE. THEY CARRY A DEPARTMENTAL ALPHANUMERICAL IDENTIFICATION.**
- 3. TECHNICAL MEMORANDA, AN INFORMAL SERIES, CONTAIN TECHNICAL DOCUMENTATION OF LIMITED USE AND INTEREST. THEY ARE PRIMARILY WORKING PAPERS INTENDED FOR INTERNAL USE. THEY CARRY AN IDENTIFYING NUMBER WHICH INDICATES THEIR TYPE AND THE NUMERICAL CODE OF THE ORIGINATING DEPARTMENT. ANY DISTRIBUTION OUTSIDE DTNSRDC MUST BE APPROVED BY THE HEAD OF THE ORIGINATING DEPARTMENT ON A CASE-BY-CASE BASIS.**